Characteristics of single and two-phase flows through porous particle beds

Jong Seok Oh [a], Sang Mo An [b], Hwan Yeol Kim [b], Min Gu Kang [a], Dong Eok Kim [a*]
[a]*School of Energy System Engineering, Chung-Ang University, Seoul 06974, Korea*
[b]*Korea Atomic Energy Research Institute, 111, Deadeok-daero 989 beon-gil, Yuseong-gu, Daejeon 34057, Korea*
**Corresponding author: dekim@cau.ac.kr*

1. Introduction

Fluid flow behaviors through porous particle beds are crucial for the safety analysis of a nuclear power reactor under severe accident condition. In this study, we conducted the single- and two-phase flow experiments through the porous beds filled with spherical particles. From the experiments, the pressure loss for single- and two-phase flows through the particle beds were measured, and counter-current flooding limit (CCFL) was found from the two-phase flow experiments. The results were analyzed using the existing models [1-4] and numerical codes. Particularly in the present study, we examined the effective particle diameter concept to model the behaviors of two-phase pressure through various non-uniform particle beds.

2. Methods

2.1 Experimental

Fig. 1 shows the schematic of the experimental facility for single- and two-phase flow experiments through the porous particle beds. Air and water at atmospheric pressure were used as working fluids. The test section was made of a transparent acrylic pipe with an inner diameter of 100 mm and height of 500 mm. The pressure drops through the test section were measured by three differential pressure transmitters with different measurement ranges of 0-1.5 kPa, 0-37.3 kPa, and 0-186.5 kPa. The flow rates of air and water were measured using a thermal mass flowmeter and elecro-magnetic flowmeter, respectively. The inlet temperature and pressure were measured using K-type thermocouples and absolute pressure transmitter (range: 0-1500 kPa). The experimental data were recorded with the sampling rate of 1 Hz.

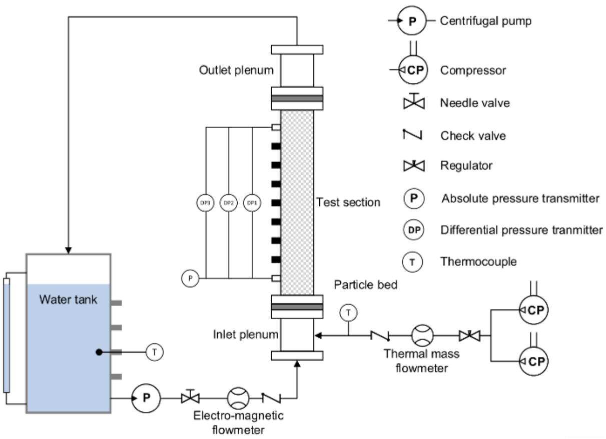

Fig. 1. Schematic of experimental facility.

The test section was filled with spherical STS304 particles to form the porous particle beds. For observing the effects of particle diameter (d_p), porosity (ε), and non-uniformity of the particle diameter, various types of particle beds were examined in the present study. Table I shows the experimental cases and specifications of the particle beds. Both uniform and non-uniform particle beds formed using the spherical particles with various diameters. For the non-uniform particle beds, two or three particles were mixed in the same mass fraction.

Table I: Experimental cases and specifications of the particle beds

Case	Working fluid	d_p (mm)	ε
1P-DP1-A		1	0.413
1P-DP3-A		3	0.398
1P-DP5-A	Single-phase Air	5	0.402
1P-DP6-A		6	0.397
1P-DP8-A		8	0.407
1P-DP1-W		1	0.411
1P-DP3-W		3	0.398
1P-DP5-W		5	0.401
1P-DP6-W		6	0.396
1P-DP8-W		8	0.405
1P-DP1/3-W		1, 3	0.356
1P-DP1/5-W		1, 5	0.320
1P-DP1/8-W	Single-phase Water	1, 8	0.290
1P-DP3/6-W		3, 6	0.371
1P-DP3/8-W		3, 8	0.358
1P-DP5/8-W		5, 8	0.392
1P-DP3/5/8-W		3, 5, 8	0.357
1P-DP3/6/8-W		3, 6, 8	0.355
1P-DP5/6/8-W		5, 6, 8	0.397
2P-DP1-AW		1	0.400
2P-DP3-AW		3	0.397
2P-DP5-AW		5	0.403
2P-DP6-AW		6	0.398
2P-DP8-AW		8	0.405
2P-DP3/6-AW	Two-phase Air/Water	3, 6	0.371
2P-DP3/8-AW		3, 8	0.358
2P-DP5/8-AW		5, 8	0.392
2P-DP3/5/8-AW		3, 5, 8	0.357
2P-DP3/6/8-AW		3, 6, 8	0.355
2P-DP5/6/8-AW		5, 6, 8	0.397

2.2 Models and numerical methods for analyzing the experimental data

For the single-phase flow cases, we adopted the Ergun's equation [1] shown in Eqs. (1) and (2).

$$-\frac{dP}{dz} = \rho_f g + \frac{\mu_f}{K} V_{sf} + \frac{\rho_i}{\eta} V_{sf} \left| V_{sf} \right|, \quad (1)$$

$$K = \frac{\varepsilon^3 d_p^2}{C_1 (1-\varepsilon)^2}, \; \eta = \frac{\varepsilon^3 d_p}{C_2 (1-\varepsilon)}, \quad (2)$$

where P, z ρ_f, g, μ_f, K, η, V_{sf}, ε, and d_p are the fluid pressure, one-dimensional coordinate in upward direction, fluid density, gravity acceleration, dynamic viscosity, permeability, passability, fluid superficial velocity, porosity, and particle diameter, respectively. C_1 and C_2 set to 150 and 1.75 given from the original Ergun correlation. For the two-phase flow cases, one-dimensional steady-state momentum equations for the gas and liquid phases can be given as Eqs. (3) and (4).

$$-\frac{dP_g}{dz} = \rho_g g + \frac{\mu_g}{KK_{rg}} V_{sg} + \frac{\rho_g}{\eta \eta_{rg}} V_{sg} \left| V_{sg} \right| + \frac{F_i}{\alpha}, \quad (3)$$

$$-\frac{dP_l}{dz} = \rho_l g + \frac{\mu_l}{KK_{rl}} V_{sl} + \frac{\rho_l}{\eta \eta_{rl}} V_{sl} \left| V_{sl} \right| - \frac{F_i}{1-\alpha}, \quad (4)$$

where K_r, η_r, F_i, α, subscripts g and l are the relative permeability, relative passability, interfacial drag force (unit: N/m^3), void fraction, gas and liquid, respectively. In the previous models [2-10], different types of the relations for K_r, η_r, and F_i were applied into Eqs. (3) and (4) depending on the relevant flow regime. In this study, we adopted three types of the models for the two-phase pressure loss through the porous particle beds, i.e., Schulenberg and Müller model [3] (SM model), Tung and Dhir model [4] (TD model), and Schmidt model [2] (SC model). We developed the in-house codes written in MATLAB R2020a for solving the pressure balance equation from Eqs. (3) and (4), i.e., $dP_g / dz = dP_l / dz$, based on the SM, TD, and SC models.

3. Results and discussion

3.1 Single-phase flow through the porous beds

In Fig. 2(a), the experimental data for the single-phase pressure gradient of air and water flows through the uniform particle beds are compared with the predictions by the Ergun's correlation [1] (Eq. (1)). The prediction results agree well with the experimental data in both qualitative and quantitative ways. The root mean square errors (E_{rms} , Eq. (5)) of the Ergun model to the experimental data for the air and water flows were calculated as 19.4% and 17.3%, respectively.

$$E_{rms} = \sqrt{\frac{1}{N} \sum_{n=1}^{N} \left(\frac{V_n^{\exp} - V_n^{\text{model}}}{V_n^{\exp}} \right)^2} \times 100 \; (\%), \quad (5)$$

where N, $V^{\exp}$, V^{model}, and n are the total number of the experimental data, experimentally measured value, predicted value by the model, and index of the data, respectively. For the non-uniform particle beds, we found the optimal particle diameter (d_{opt}) using the least square fitting method with the Ergun correlation, and the calculated values of d_{opt} for the experimental cases shown in Fig. 2(b). As shown in Fig. 2(b), the Ergun correlation using d_{opt} predicted well the experimental data for the non-uniform particle beds ($E_{rms} = 20.2\%$). Thus, the values of d_{opt} are used as the effective particle diameters for the analyses of two-phase pressure loss through the non-uniform particle beds.

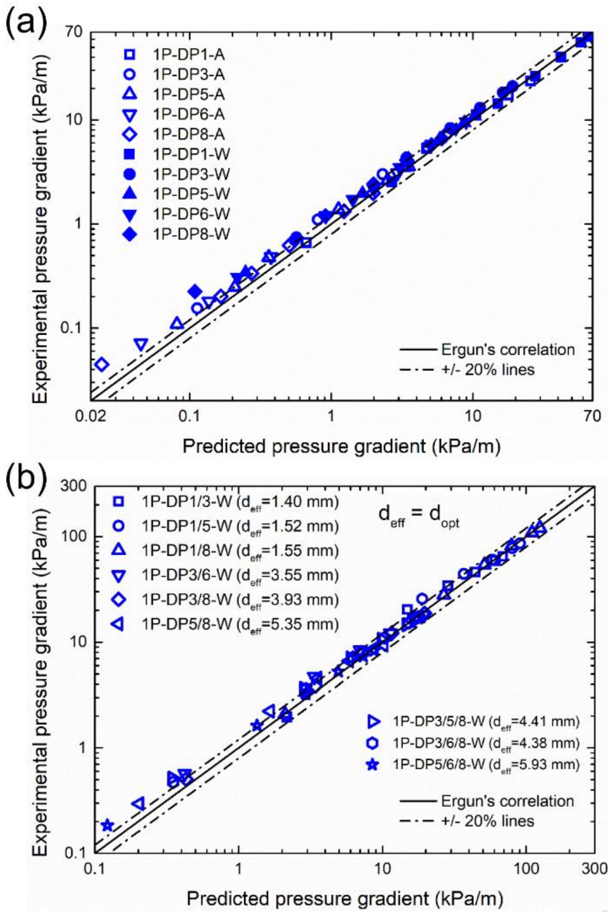

Fig. 2. Comparison of the experimental single-phase pressure gradient data and predictions from the Ergun correlation for (a) the uniform and (b) non-uniform particle beds.

3.2 Two-phase flow through the porous beds

Fig. 3 shows the experimental data and prediction results for the two-phase pressure loss through the uniform particle beds. The pressure loss data are represented by the non-dimensional pressure gradient P^* (Eq. (6)).

$$P^* = \frac{-dP/dz}{g(\rho_l - \rho_g)}. \quad (6)$$

As shown in Fig. 3, the three models predict well the trend of P^* decrease at the initial low gas flow rate. The reduction of P^* at low V_{sg} is caused by the action of gas-liquid interfacial drag force. The SM and SC models predicted well the increase of P^* followed by its reduction at low gas flow rate, however, the TD model did not properly simulate the recovery of P^* at the moderate gas flow rate. Moreover, the TD model significantly underestimated the experimental P^* in the moderate and high V_{sg} range. We consider that the effect of the interfacial drag force is overestimated in the TD model. Fig. 4 shows the comparisons between the experimental P^* data and model predictions for the non-uniform particle beds. For the model calculation, the effective particle diameters in Fig. 2(b) were used. Similarly in the uniform particle bed cases, the SM and SC models predicted well the behaviors of the experimental pressure loss, while the TD model significantly underestimated the experimental data in the moderate and high V_{sg} range. As a result, the values of E_{rms} for the SM, TD, and SC models were calculated to 7.7%, 25.5%, and 5.4%, respectively.

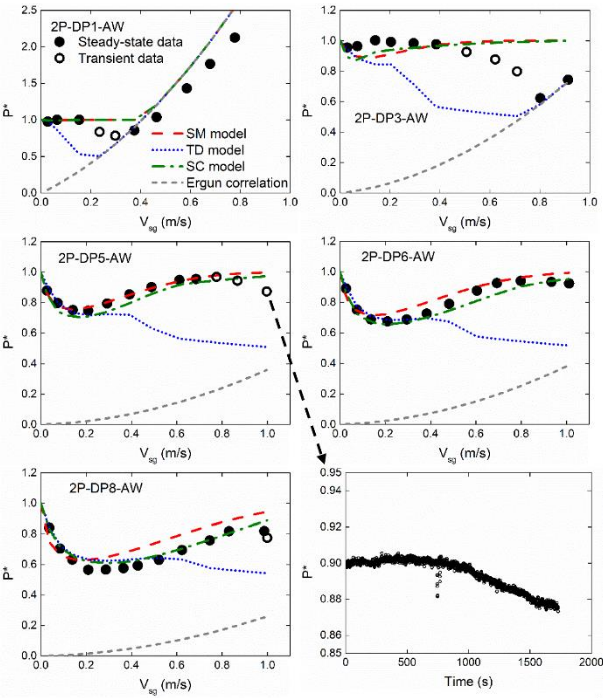

Fig. 3. Experimental P^* data and model predictions for the uniform particle bed cases.

In Figs. 3 and 4, the experimental P^* data are classified into steady-state (black circles) and transient (hollow circles) data. In the transient data points, the experimental pressure loss through the particle beds did not reach the steady-state and showed the behaviors of long-term (more than 1 hour) variation shown in Fig. 3. And, the dryout phenomenon in the particle bed was experimentally observed at the points, i.e., the CCFL triggers. At the CCFL points, the P^* lines predicted from the models should graphically overlap with the lines by the Ergun correlation. As shown in Figs. 3 and 4, the adopted models largely overestimated the experimental CCFL points. Since the CCFL can act as a trigger of dryout phenomenon of the debris bed followed by loss of coolability for the fuel particles under a severe accident condition, a reliable prediction of the CCFL phenomenon is crucial to the nuclear safety application. It is recommended as a future work.

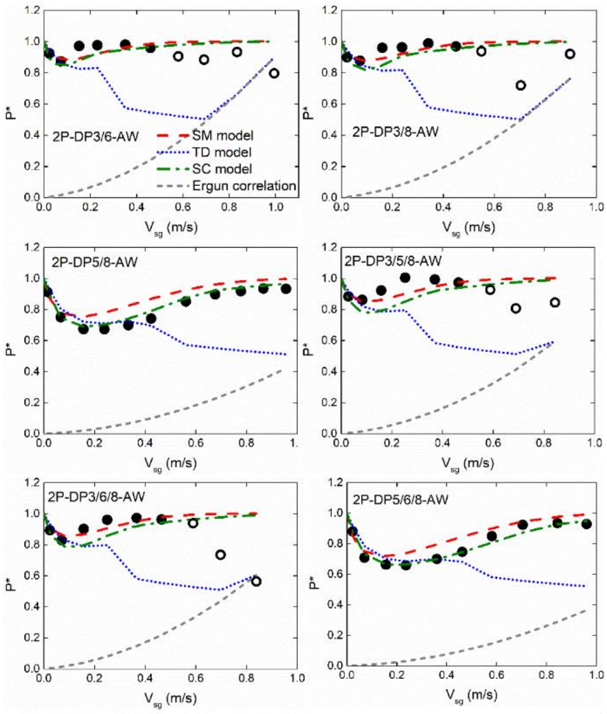

Fig. 4. Experimental P^* data and model predictions for the non-uniform particle bed cases.

4. Conclusions

The results of this study can be summarized as below:

- The pressure drop data in single-phase flow experiments for the uniform particle beds showed good agreements with the original Ergun correlation within ±20%.
- For the non-uniform particle beds, the experimental single-phase pressure loss data could be fitted well with the Ergun correlation using the effective particle diameter obtained from least square fitting method.
- The predictability of the previous models for the two-phase experimental data relied strongly on their sub-models of interfacial drag force.
- The SM and SC models predicted reasonably well the overall two-phase pressure loss for the uniform and non-uniform particle beds, while the TD model significantly underestimated the experimental data at moderate and high V_{sg} range.
- In the experiments, the CCFL phenomenon was observed, and the models overestimated the experimental CCFL points. Thus, a future work is recommended.

ACKNOWLEDGEMENT

This work was supported by the Korean Institute of Energy Technology Evaluation and Planning (KETEP) granted financial resource from the Ministry of Trade, Industry & Energy, Republic of Korea (No. 20193110100090).

REFERENCES

[1] S. Ergun, Fluid flow through packed columns, Chem. Eng. Prog. Vol. 48, pp. 89-94, 1952.
[2] W. Schmidt, Influence of multidimensionality and interfacial friction on the coolability of fragmented corium, Ph. D. Thesis, Univ. Stuttgart, 2004.
[3] T. Schulenberg, U. Müller, An improved model for two-phase flow through beds of coarse particles, Int. J. Multiphas. Flow Vol. 13, pp. 87-97, 1987.
[4] V.X. Tung, V.K. Dhir, A hydrodynamic model for two-phase flow through porous media, Int. J. Multiphas. Flow Vol. 14, pp. 47-65, 1988.
[5] K. Hu, T.G. Theofanous, On the measurement and mechanism of dryout in volumetrically heated coarse particle beds, Int. J. Multiphas. Flow, Vol. 17, pp. 519-532, 1991.
[6] R.J. Lipinski, A model for boiling and dryout in particle beds, No. NUREG/CR-2646, Sandia National Labs., 1982.
[7] N.K. Tutu, T. Ginsberg, J.C. Chen, Interfacial drag for two-phase flow through high permeability porous beds, J. Heat Transfer, Vol. 106, pp. 865-870, 1984.
[8] A.S. Naik, V.K. Dhir, Forced flow evaporative cooling of a volumetrically heated porous layer, Int. J. Heat Mass Tran., Vol. 25, pp. 541-552, 1982.
[9] J.H. Park, H.S. Park, M. Lee, K. Moriyama, Modeling of pressure drop in two-phase flow of mono-sized spherical particle beds, Int. J. Heat Mass Tran., Vol. 127, pp. 986-995, 2018.
[10] D.Y. Yeo, H.C. No, A zero-dimensional dryout heat flux model based on mechanistic interfacial friction models for two-phase flow regimes with channel flow in a packed bed, Int. J. Heat Mass Tran. Vol. 141, pp. 554-568, 2019.